

# Aqueous-phase biphasic dehydroaromatization of bio-derived limonene into *p*-cymene by soluble Pd nanocluster catalysts

Chen Zhao<sup>a</sup>, Weijia Gan<sup>a</sup>, Xiaobing Fan<sup>a</sup>, Zhipeng Cai<sup>a</sup>, Paul J. Dyson<sup>b,\*</sup>, Yuan Kou<sup>a,\*</sup>

<sup>a</sup> PKU Green Chemistry Center, Beijing National Laboratory for Molecular Sciences, College of Chemistry and Molecular Engineering, Peking University, Beijing 100871, China

<sup>b</sup> Institut des Sciences et Ingénierie Chimiques, Ecole Polytechnique Fédérale de Lausanne (EPFL), CH-1015 Lausanne, Switzerland

Received 19 October 2007; revised 24 December 2007; accepted 2 January 2008

Available online 31 January 2008

## Abstract

A biphasic approach to the dehydroaromatization of bioderived limonene into water-insoluble *p*-cymene using soluble Pd nanoparticle catalysts in an aqueous phase ( $\geq 150$  °C, 2 bar H<sub>2</sub>) was successfully achieved with a conversion of 93% and a selectivity of 82%. The Pd nanoparticles, operating under forcing conditions (180 °C, 2 bar H<sub>2</sub>), can be recycled at least four times without noticeable degradation. The effects of temperature, pressure, reaction time, pH, catalyst concentration, metal type, the type and amount of polymer stabilizer, and the preparation method were systematically investigated to optimize the process and provide insight into the mechanisms involved.

© 2008 Elsevier Inc. All rights reserved.

**Keywords:** Limonene; *p*-Cymene; Dehydroaromatization; Palladium; Nanoparticles; Biphasic catalysis; Terpene; Poly(*N*-vinyl-2-pyrrolidone); Biomass

## 1. Introduction

The conversion of natural biomass materials (e.g., terpenes) to value-added chemical and fine chemical products, as recently described by Corma et al. [1], is highly important, and such conversion via green catalytic processes remains a considerable challenge. Limonene is a waste product obtained in vast quantities from the fruit juice industry. Because limonene is a fragrant active mono-terpene and renewable feedstock, its conversion to the valuable aromatic compound *p*-cymene is of great commercial interest [2,3].

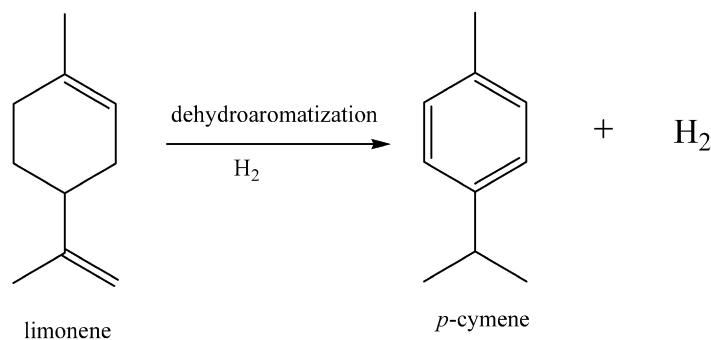
The dehydroaromatization of limonene to *p*-cymene under a hydrogen atmosphere (Scheme 1) comprises a relatively complex series of reactions. Hydrogenation, dehydrogenation, and isomerization reactions occur simultaneously, making it difficult to obtain a single product with high selectivity. The dehydroaromatization of limonene to *p*-cymene over heterogeneous catalysts, such as Pd/SiO<sub>2</sub> [4,5], Pd/zeolite [6,7], Pd/C,

Pd/Al<sub>2</sub>O<sub>3</sub> [8], Pt/Al<sub>2</sub>O<sub>3</sub> [9], Pt/C [10], Cu–Ni [11], and heteropolyacid H<sub>5</sub>PMo<sub>10</sub>V<sub>2</sub>O<sub>40</sub> [12], has been investigated in detail. From these studies, it appears that palladium-based catalysts are the most efficient; for example, selectivities of 70% over Pd/C [8] and 90% over Pd/SiO<sub>2</sub> were obtained using H<sub>2</sub> as carrier gas on a fixed-bed reactor [4,5].

Environmentally benign water-based systems using metallic nanoparticles as catalysts have not yet been reported. Aqueous–organic biphasic systems offer certain advantages for the separation of products, such as water-insoluble *p*-cymene, from hydrophilic catalysts [13,14]. Immobilization of a nanoparticle catalyst in water rather than on a surface allows all of the surface atoms of the nanoparticle to may participate in catalysis, thereby permitting a traditional gas–solid phase heterogeneous catalytic process at the gas–liquid–solid interface [15]. Aqueous-phase processes also facilitate the controlled supply or dissipation of heat in reactions. In previous work, we found that soluble nanoparticle catalysts exhibited high catalytic activity under mild conditions; examples include Ru nanoparticles catalyzing the selective hydrogenation of cellobiose in water [16], Rh nanoparticles catalyzing the hydrogenation of benzene [17] and arenes [18] in ionic liquids, Pt nanoparticles selectively catalyzing the hydrogenation of

\* Corresponding authors. Faxes: +41 21 693 98 85, +86 10 62751708.

E-mail addresses: [paul.dyson@epfl.ch](mailto:paul.dyson@epfl.ch) (P.J. Dyson), [yankou@pku.edu.cn](mailto:yankou@pku.edu.cn) (Y. Kou).



Scheme 1. Dehydroaromatization of limonene to *p*-cymene under a hydrogen atmosphere.

*o*-chloronitrobenzene [19] and cinnamaldehyde [20] in ionic liquids, and Pt nanoparticles catalyzing the aerobic oxidation of alcohols in aqueous–organic biphasic systems [21]. Among these, aqueous–organic [21] and ionic liquid–organic systems [17–20] have shown great potential in reaction control and product separation.

In general, however, soluble nanoparticles are not thermally stable at higher temperatures [22]. The highest working temperature reported to date is 160 °C for Pd-catalyzed Heck coupling reactions [23]. Herein we report for the first time that soluble Pd nanoparticles can efficiently catalyze the dehydroaromatization of limonene to *p*-cymene at 180 °C under 2 bar H<sub>2</sub> in an aqueous solution. After reaction, the *p*-cymene and the nanoparticle-containing aqueous solution are separated into two phases. The catalyst may be reused several times without deactivation after reaction at 180 °C. We also characterize the relationship between the nanoparticles' structure and their activity and stability.

## 2. Experimental

### 2.1. General procedures

Limonene (boiling point, 176–178 °C; purity, 98% [GC]) was provided by Nanjing Huagong Co, Ltd., China. RuCl<sub>3</sub>, H<sub>2</sub>PtCl<sub>6</sub>, PdCl<sub>2</sub>, RhCl<sub>3</sub>, and HAuCl<sub>4</sub> (all AR grade) were obtained from Shenyang Research Institute of Nonferrous Metals, China. Poly(*N*-vinyl-2-pyrrolidone) (PVP) with various alkyl chain lengths (i.e., K15, K30, K60, K90; average  $M_w$  = 10,000, 30,000, 220,000, and 630,000, respectively) were purchased from J & K Chemicals Ltd. *N,N*-dimethyl-*N*-cetyl-*N*-(2-hydroxyethyl)-ammonium bromide was synthesized as described previously [24]. Ethanol (GR grade) was refluxed with state agent and distilled under nitrogen (99.9995%) before use. All other chemicals were used as received without further purification.

Gas chromatography (GC) analysis was performed using an Agilent 6820 gas chromatograph with a flame ionization detector equipped with a 30 m (0.25-mm-i.d.) HP Innowax column. GC–mass spectroscopy (GC–MS) analysis was performed using an Agilent GC 6890 with an Agilent 5973 *inert* mass selective detector.

### 2.2. Catalyst preparation

#### 2.2.1. Nanoparticle synthesis using ethanol–water reduction [25]

Aqueous solutions of PVP-metal nanoparticles were prepared from the appropriate metal salt and PVP-K15, -K30, -K60, or -K90. In a typical reaction, PdCl<sub>2</sub> was converted to H<sub>2</sub>PdCl<sub>4</sub>–H<sub>2</sub>O using hydrochloric acid, after which the H<sub>2</sub>PdCl<sub>4</sub>–H<sub>2</sub>O solution ( $C_{\text{Pd}} = 0.0221$  mol/L, 1.4 mL, 0.03 mmol) and PVP (0.062 g, 0.6 mmol) were added to a mixture of H<sub>2</sub>O (30 mL) and ethanol (30 mL). The solution was stirred under reflux at 80 °C for 2 h, during which time it turned black. The solvent was removed in vacuo, and distilled water (30 mL) was added to form a Pd nanoparticle solution in water ( $C_{\text{Pd}} = 10^{-3}$  mol/L). Other metal nanoparticles were prepared in the same way but using different precursors (i.e., RuCl<sub>3</sub>, H<sub>2</sub>PtCl<sub>6</sub>, RhCl<sub>3</sub> and HAuCl<sub>4</sub>).

#### 2.2.2. Nanoparticle synthesis using H<sub>2</sub> reduction

Typically, an H<sub>2</sub>PdCl<sub>4</sub>–H<sub>2</sub>O solution ( $C_{\text{Pd}} = 0.0221$  mol/L, 1.4 mL, 0.03 mmol) and PVP (0.124 g, 1.2 mmol) were mixed in H<sub>2</sub>O (30 mL). The solution was reduced in an autoclave under H<sub>2</sub> (40 bar) at 100 °C for 3 h to form a Pd nanoparticle solution.

#### 2.2.3. Nanoparticle synthesis using NaBH<sub>4</sub> reduction [24]

PVP (0.670 g, 6.6 mmol) or *N,N*-dimethyl-*N*-cetyl-*N*-(2-hydroxyethyl)-ammonium bromide (0.260 g, 0.66 mmol) was dissolved in H<sub>2</sub>O (45 mL), and then sodium borohydride (36 mg, 0.95 mmol) was added. This mixture was added, with vigorous agitation, to an aqueous solution of H<sub>2</sub>PdCl<sub>4</sub> ( $C_{\text{Pd}} = 0.0221$  mol/L, 15 mL) to give Pd nanoparticles.

### 2.3. Limonene conversion using the nanoparticle solutions

In a typical reaction, limonene (1.36 g, 0.01 mol) and the metal nanoparticles in water (10 mL,  $1 \times 10^{-3}$  mol) were added to an autoclave (reactor volume, 100 mL). The reaction was carried out under 2 bar H<sub>2</sub> at 150 °C for 3 h at a stirring speed of 500 rpm. After reaction, the products and the nanoparticle solution were separated into two phases, and the upper organic product layer was collected and analyzed by GC and GC–MS.

## 2.4. Catalyst recycling experiments

The Pd nanoparticle solution (60 mL,  $5 \times 10^{-3}$  mol), synthesized by ethanol–water reduction and stabilized by PVP-K90, was mixed with limonene (2.04 g, 0.015 mol). This mixture was added to the autoclave and reacted at 180 °C under 2 bar H<sub>2</sub> for 3 h. After reaction, the upper organic layer was decanted and analyzed by GC and GC–MS, and the recovered Pd nanoparticles were reused with no further treatment.

## 2.5. Determination of Pd leaching by inductively coupled plasma-atomic emission spectroscopy

The Pd content in the organic phase was determined by inductively coupled plasma-atomic emission spectroscopy (ICP-AES). The organic phase was removed under vacuum, and HNO<sub>3</sub> (10 mL) and HCl (30 mL) were added to the residue. The mixture was heated at 100 °C for 12 h until the Pd metal was thoroughly dissolved. The resulting transparent solution was diluted to 500 mL with deionized water and analyzed by ICP-AES (Profile Spec, Leeman Labs; detection limit, 1 µg–mg/mL).

## 2.6. Nanoparticle characterization by transmission electron microscopy

Transmission electron microscopy (TEM) was performed with a Hitachi H-9000 HRTEM at 300 keV. The nanoparticles were diluted in methanol, and one drop of solution was placed on a copper grid coated with carbon film. To determine the size distribution, more than 300 particles were counted from each sample.

## 3. Results and discussion

### 3.1. Dehydroaromatization of limonene under different conditions

To find a suitable catalyst for the conversion of limonene to *p*-cymene, nanoparticle catalysts composed of five different transition metals (i.e., Pd, Rh, Ru, Pt, and Au) were prepared and evaluated under the same conditions (150 °C, 2 bar H<sub>2</sub>, 1 h). The metal nanoparticles were prepared by ethanol–water reduction of the appropriate metal salts with PVP. Among these, the Au nanoparticles demonstrated very low activity, possibly due, at least in part, to their instability under the reaction conditions. Au deposits were observed along with a colorless solution at the end of the reaction. Pt, Ru, and Rh all exhibited good activity in the reaction but with poor selectivity (<10%). Only the Pd nanoparticles exhibited high stability under the reaction conditions and gave relatively high activity and selectivity, that is, a conversion of 70% with a selectivity of 25% toward the *p*-cymene product. It is interesting that Pd nanoparticles prepared by other methods also have demonstrated very good selectivity in previous studies [26–28].

Temperature, hydrogen pressure, and reaction time were evaluated to optimize the reaction conditions. The temperature was varied from 100 to 200 °C and was found to have

a pronounced effect on the reaction. Isomerization and dehydrogenation reactions are endothermic, and, as expected, the selectivity toward *p*-cymene increased with temperature; for example, a selectivity of 9.3% was observed at 120 °C, increasing to 33% at 150 °C over the same Pd nanoparticle catalyst. The selectivity of *p*-cymene should be sensitive to hydrogen pressure, because 1 mol of hydrogen is released during the dehydrogenation of limonene. Preliminary results showed that the selectivity increased from 4.2 to 58% as the hydrogen pressure was reduced from 40 to 0 bar; however, Pd nanoparticles were not stable in an N<sub>2</sub> atmosphere without H<sub>2</sub>, indicating that the H<sub>2</sub> atmosphere helps stabilize the Pd nanocatalysts, especially at higher temperatures. In addition, under lower pressure of H<sub>2</sub> (2 bar), the reaction reached equilibrium in 2–3 h, and a turnover frequency (TOF) > 700 h<sup>-1</sup> was maintained.

For the Pd nanoparticle catalysts operating in aqueous solutions, acidic (pH 2) or neutral (pH 7) solutions gave the best activity. Decreasing the pH to 0 not only eroded the stainless steel autoclave, but also led to low activity and selectivity. Although basic catalysts, such as CaO, can selectively catalyze limonene to *p*-cymene [29], high-pH (i.e., pH 10, 12, and 14) solutions containing the nanoparticle catalysts produced conversions of only ca. 30%.

A Pd concentration of 10<sup>-3</sup> mol/L was generally used in this work because this concentration yielded good selectivity with a high conversion at 150 °C. In principle, more dilute Pd solutions should facilitate control of the nanoparticle assembly process, but at the expense of catalytic activity. Three nanoparticle solutions with different Pd concentrations were evaluated, as shown in Table 1 (entries 1–3). Increasing the concentration from 0.001 to 0.005 to 0.01 mol/L led to slightly increased conversion but significantly increased selectivity. The most concentrated Pd nanoparticle solution (0.01 mol/L; entry 3) provided a selectivity of 78% with a near-quantitative conversion, although the reaction rate (TOF) was reduced to 96 h<sup>-1</sup>.

Table 1  
Conversion of limonene using soluble Pd nanoparticles under different conditions<sup>a</sup>

Entry	<i>T</i> (°C)	Time (h)	PVP type	Pd concentration (mol/L)	Conversion (GC-%)	<i>p</i> -Cymene selectivity (GC-%)	TOF (h <sup>-1</sup> ) <sup>b</sup>
1 <sup>c</sup>	180	3	K30	0.001	91	44	677
2 <sup>c</sup>	180	3	K30	0.005	99	70	195
3 <sup>c</sup>	180	3	K30	0.01	96	78	96
4	150	3	K15	0.001	92	31	720
5	150	3	K30	0.001	94	32	750
6	150	3	K60	0.001	93	25	710
7	150	3	K90	0.001	82	26	730
8 <sup>c</sup>	180	1	K15	0.001	97	49	970
9 <sup>c</sup>	180	1	K30	0.001	68	32	677
10 <sup>c</sup>	180	1	K60	0.001	74	38	735
11	180	1	K90	0.001	74	45	741

<sup>a</sup> General conditions: PVP:Pd (mol:mol) = 20, Pd ( $1 \times 10^{-3}$  mol/L, 10 mL), nanoparticles were synthesized by alcohol–water reduction, water as solvent, pH 2, limonene (1.360 g, 0.01 mol), 2 bar H<sub>2</sub>, stirred at 500 rpm.

<sup>b</sup> Tested after 1 h, defined as number of moles of consumed H<sub>2</sub> per mole of Pd per hour, determined by GC.

<sup>c</sup> Nanoparticle aggregation observed.

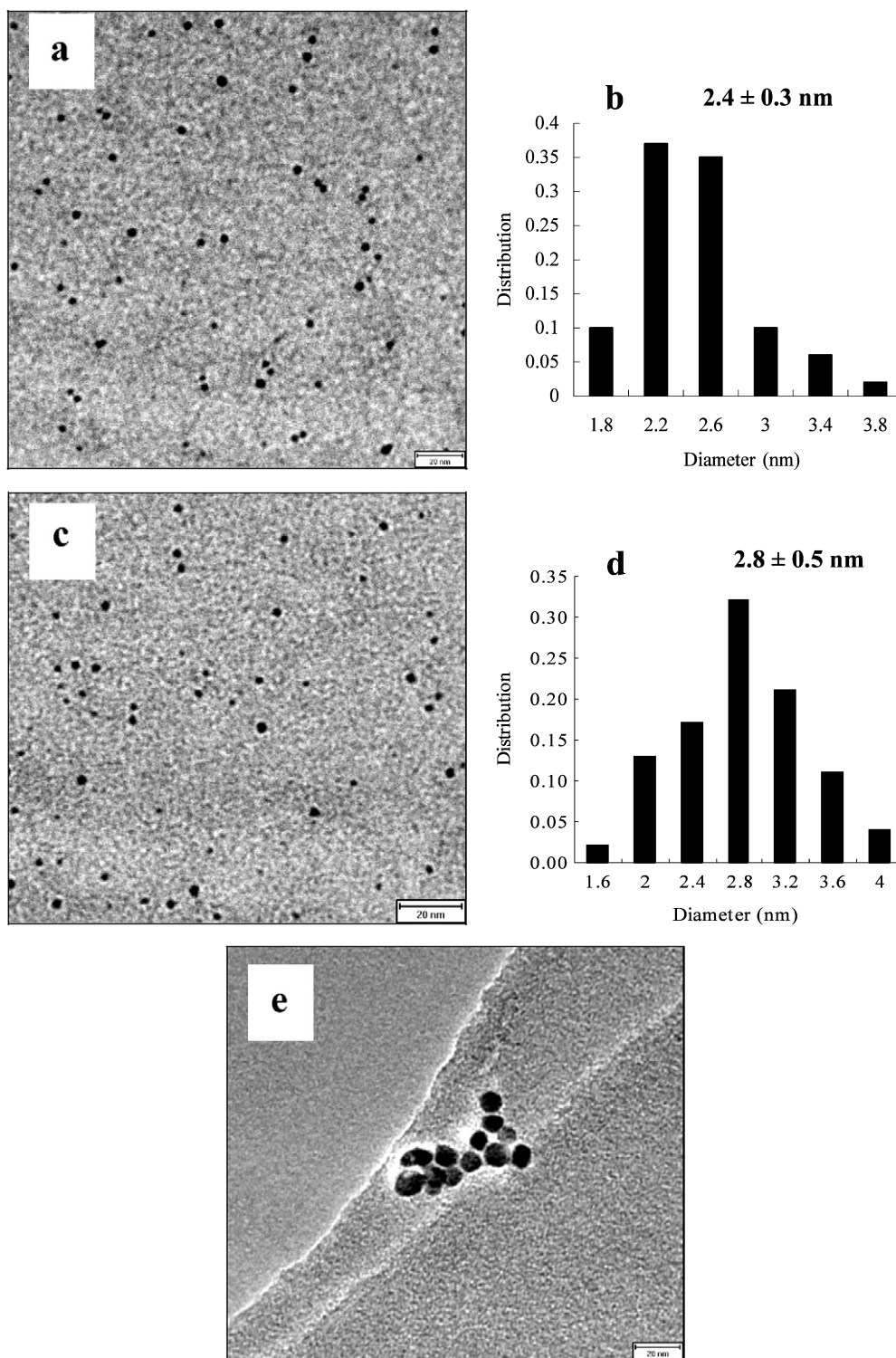


Fig. 1. (a) TEM micrograph of Pd nanoparticles protected by PVP-K90 in water before catalysis (scale bar = 20 nm). Nanoparticles were synthesized according to the method described in Section 2.2.1. (b) Histogram showing the particle size distribution from (a). (c) TEM micrograph of Pd nanoparticles after the first run of recycling experiment, as described in Section 2.4. Scale bar = 20 nm. (d) Histogram showing the particle size distribution from (c). (e) TEM micrograph of Pd nanoparticles stabilized by PVP-K15 after reaction under 2 bar  $H_2$  at 180 °C for 3 h, stirred at 500 rpm,  $[Pd] = 5 \times 10^{-3}$  mol/L, limonene/catalyst = 50/1 mol/mol. Scale bar = 20 nm.

Four different PVP polymers with various alkyl chain lengths (i.e., K15, K30, K60, and K90, with average  $M_w = 10,000, 30,000, 220,000,$  and  $630,000$ , respectively) were evaluated under relatively mild conditions (150 °C, 2 bar  $H_2$ , 3 h).

Table 1 (entries 4–7) shows that the overall catalytic efficiencies of the Pd nanoparticles protected by these four types of PVP were essentially the same. However, under more severe conditions (i.e., 180 °C), the lower molecular weight polymers (i.e.,



Table 2  
Conversion of limonene using hydrogen acceptors and/or using different Pd nanoparticle preparation methods<sup>a</sup>

Entry	Stabilizer	Preparation method	<i>T</i> (°C)	Stabilizer/Pd (mol/mol)	Substrate/Pd (mol/mol)	Conversion (GC-%)	<i>p</i> -Cymene selectivity (GC-%)	TOF (h <sup>-1</sup> ) <sup>b</sup>
1 <sup>c</sup>	PVP-K30	H <sub>2</sub> reduction	150	40	1000	89	22	705
2 <sup>c</sup>	PVP-K90	H <sub>2</sub> reduction	180	20	1000	68	29	620
3 <sup>c</sup>	PVP-K30	NaBH <sub>4</sub> reduction	180	20	200	99	66	170
4 <sup>c</sup>	Surfactant	NaBH <sub>4</sub> reduction	180	2	200	97	70	160
5 <sup>c</sup>	PVP-K30	Alcohol water reduction	180	100	1000	93	52	910
6	PVP-K90	Alcohol water reduction	180	100	1000	89	34	850
7 <sup>c</sup>	PVP-K15	Alcohol water reduction	180	20	200	98	77	158
8 <sup>c</sup>	PVP-K30	Alcohol water reduction	180	20	200	99	70	180
9	PVP-K90	Alcohol water reduction	180	20	200	99	70	180
10 <sup>d</sup>	PVP-K90	Alcohol water reduction	180	20	50	93	82	46
11 <sup>d</sup>	PVP-K90	Alcohol water reduction	180	20	50	99	87	50
12 <sup>d</sup>	PVP-K90	Alcohol water reduction	180	20	50	85	81	30
13 <sup>d</sup>	PVP-K90	Alcohol water reduction	180	20	50	90	70	40

<sup>a</sup> General conditions: 2 bar H<sub>2</sub>, 3 h, stirred at 500 rpm, Pd (1 × 10<sup>-3</sup> mol/L, 10 mL in entries 1–6; 5 × 10<sup>-3</sup> mol/L, 20 mL in entries 7–9), water as solvent, pH 2.

<sup>b</sup> Determined after 1 h, defined as number of moles of consumed H<sub>2</sub> per mole of Pd per hour, determined by GC.

<sup>c</sup> Nanoparticle aggregation observed.

<sup>d</sup> Pd (5 × 10<sup>-3</sup> mol/L, 60 mL), limonene (2.040 g, 0.015 mol), recycling data.

PVP-K15, PVP-K30, and PVP-K60) could not protect the particles against aggregation (see Table 1, entries 8–10). Clearly, there is a fine balance between stability and reactivity. For example, the Pd nanoparticles stabilized by PVP-K15 exhibited the highest activity with a TOF of 970 h<sup>-1</sup> (Table 1, entry 8), although these nanoparticles agglomerated under the reaction conditions. The Pd nanoparticles protected by the PVP-K90 were stable even at 180 °C, albeit with a lower TOF of 741 h<sup>-1</sup>.

TEM micrographs of the Pd nanoparticles with different PVP stabilizers (Figs. 1 and S1) show that the Pd nanoparticles protected by PVP-K15 contained both small and large particles, ranging in size from 2.4 to 3.2 nm. The nonuniformity of the particles can lead to good initial activity (TOF = 970 h<sup>-1</sup>) but poor stability (Fig. 1e). The Pd nanoparticles stabilized by PVP-K90 are more uniform than those protected by PVP-K15. A narrow unimodal size distribution with a diameter of 2.4 ± 0.3 nm was observed for the freshly prepared Pd nanoparticles (Figs. 1a and 1b), and a diameter of 2.8 ± 0.5 nm was observed after the catalysis (Figs. 1c and 1d). In general, it can be concluded from Fig. S1 that the smaller the Pd nanoparticle size, with a narrower size distribution, the higher the catalytic activity and stability.

Three reducing agents (i.e., H<sub>2</sub>, NaBH<sub>4</sub>, and C<sub>2</sub>H<sub>5</sub>OH) were used to prepare the Pd nanoparticles. Table 2 shows that the Pd nanoparticles reduced by H<sub>2</sub> in either pure water or ethanol–water mixture [30,31] gave the most unstable catalysts under equivalent reaction conditions, resulting in poor selectivity and pronounced aggregation. The Pd nanoparticles prepared by reduction with NaBH<sub>4</sub> in the presence of either the surfactant, *N,N*-dimethyl-*N*-cetyl-*N*-(2-hydroxyethyl)-ammonium bromide (HEA16 Br) [23], or PVP were more stable than those prepared by H<sub>2</sub> reduction, resulting in a selectivity of 70% and a conversion of nearly 100%; however, extensive aggregation of the nanoparticles also was observed after the reaction. The Pd nanoparticles obtained by reduction with ethanol gave the same results, a selectivity of 70% and a conversion of nearly 100%,

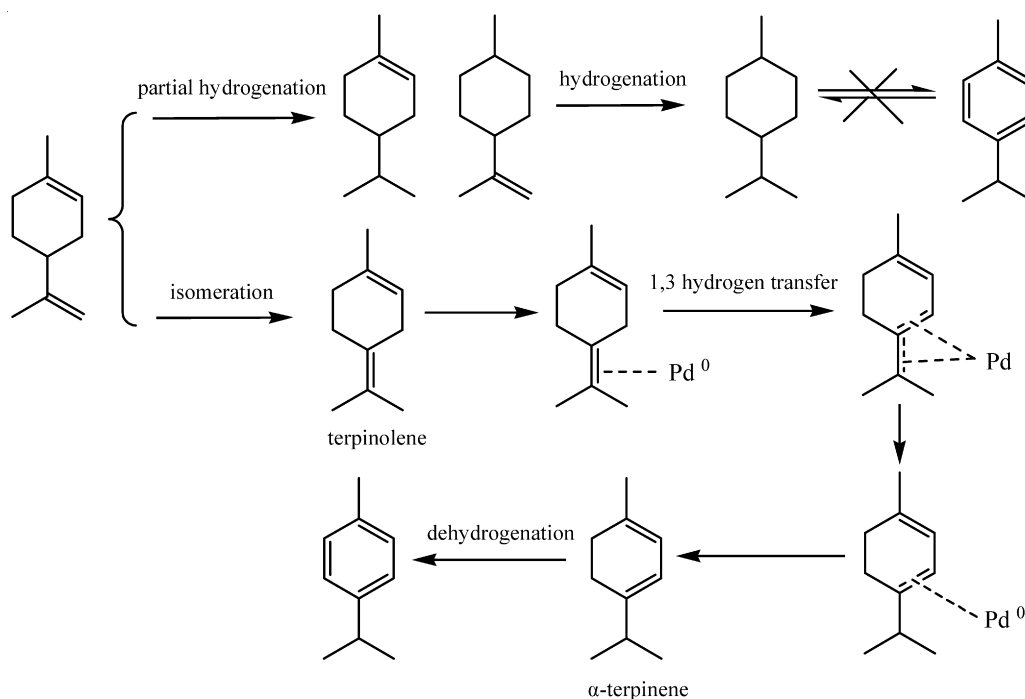
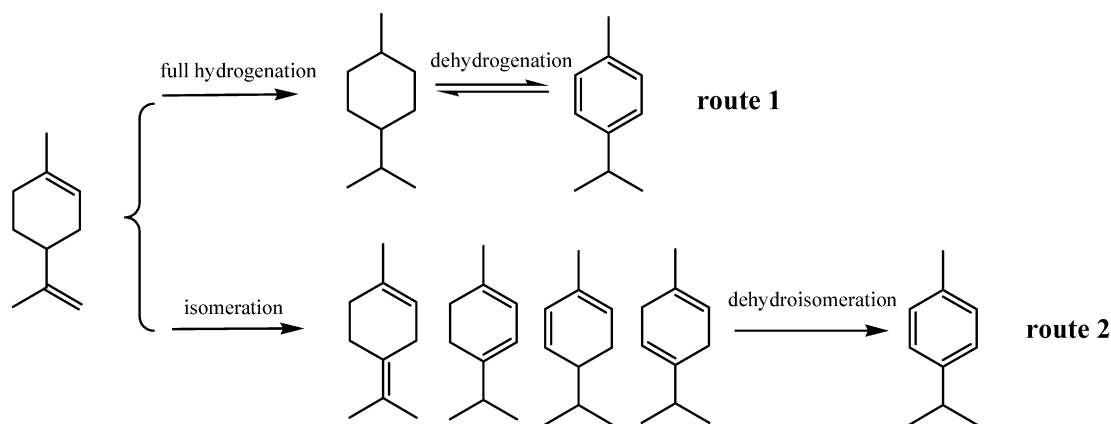
but with no aggregation observed after operating at 180 °C (Table 2, entry 9), demonstrating again that PVP-K90 was the most effective stabilizer for the nanoparticles operating at higher temperatures.

### 3.2. Catalyst recycling

To test recyclability, a Pd catalyst prepared by ethanol–water reduction and protected by PVP-90 was recycled four times at 180 °C and 2 bar H<sub>2</sub> (Table 2, entries 10–13). The biphasic approach made separation of the product very easy, and no Pd leaching was found within the detection limit (1 µg–mg/mL; standard ICP-AES analysis). The catalysts recovered in the aqueous phase were reused with no further treatment. It can be seen from Table 2 that the first run successfully reached a conversion of 93% and a selectivity of 82% (entry 10), whereas the second run successfully reached a conversion of 99% and a selectivity of 87% (entry 11). Good selectivity (ca. >80%) and near-quantitative conversion were obtained throughout the recycling.

### 3.3. Proposed mechanism for the dehydroaromatization of limonene over the Pd nanoparticles

The conversion of limonene to *p*-cymene on a Pd/SiO<sub>2</sub> heterogeneous catalyst has been proposed to occur through the dehydroaromatization mechanism shown in Scheme 2a [9]. Two reaction routes were determined by changing the catalysts and/or the carrier gas. When the Pd/SiO<sub>2</sub> catalyst and H<sub>2</sub> atmosphere were used simultaneously, the reaction was believed to follow route 1 (including full hydrogenation followed by dehydrogenation), and thus the only byproduct was the fully hydrogenated compound *p*-menthane. In the absence of Pd (i.e., simply using SiO<sub>2</sub> as catalyst), or in the case where N<sub>2</sub> was used in place of H<sub>2</sub> but still with Pd/SiO<sub>2</sub>, additional isomerization products were obtained.



Scheme 2. Proposed mechanism of limonene conversion over (a) heterogeneous Pd/SiO<sub>2</sub> and (b) soluble Pd catalysts.

Nonetheless, when we used Pd nanoparticles and H<sub>2</sub>, the reaction did not appear to involve full hydrogenation followed by dehydrogenation. This hypothesis is supported by the following observations. First, it can be seen from Fig. 2 that the increased selectivity of *p*-cymene was accompanied by a decrease in selectivity toward the isomerization products, indicating that the isomerization products were transformed mainly to *p*-cymene. Second, the Pd nanoparticles were unable to dehydrogenate *p*-menthane to *p*-cymene. When *p*-menthane was used as a substrate, even in the presence of freshly prepared Pd nanoparticles, no dehydrogenation products were observed, indicating an alternative pathway to route 1. The observation of terpinolene and  $\alpha$ -terpinolene indicates that the correspond-

ing isomerization was the main reaction pathway. The process of isomerization on the soluble Pd nanoparticles likely proceeded by a single route (i.e., the production of terpinolene and then of  $\alpha$ -terpinolene), suggesting a highly selective isomerization pathway for the nanoparticle catalysis. Thus, the Pd nanoparticles would appear to facilitate the isomerization of the double bond in a selective manner (Scheme 2b). If this were not the case, then many isomerization products other than terpinolene and  $\alpha$ -terpinolene would be produced, as has been observed over supported Pd catalysts. Based on all of these findings, we illustrate a plausible reaction pathway involving initial isomerization followed by dehydrogenation in Scheme 2b.

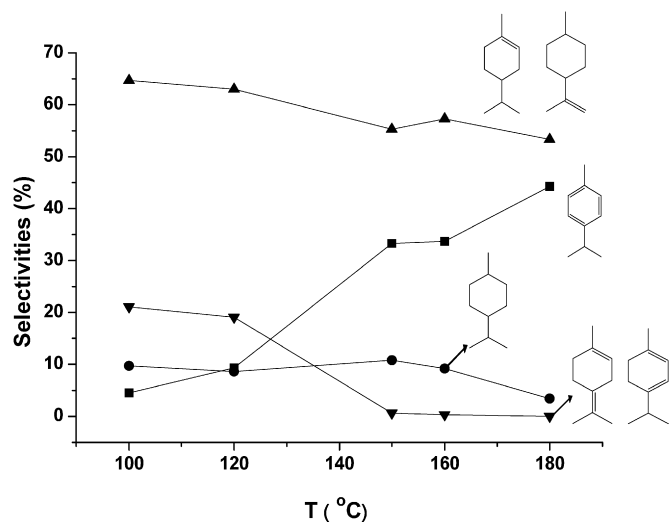


Fig. 2. Product distributions for limonene conversion as a function of temperature. Reaction conditions: Reactions were carried out in an autoclave in water containing Pd nanoparticles under 2 bar  $H_2$  for 5 h, stirred at 500 rpm. Further reaction parameters and experimental data are given in Table S1, entries 1–5.

#### 4. Conclusion

Biphasic dehydroaromatization of the renewable biomass material limonene into *p*-cymene using soluble Pd nanoparticle catalysts in aqueous solution in the presence of hydrogen occurs under severe conditions ( $\geq 150^\circ C$ ), achieving a conversion of 93% and a selectivity of 82%. The Pd nanoparticle catalysts can be recycled at least four times without deactivation even after reaction at  $180^\circ C$ . To the best of our knowledge, this is the highest operating temperature that soluble metal nanoparticles can tolerate in the liquid phase.

The effects of temperature, pressure, reaction time, pH, catalyst concentration, metal type, and stabilizer were systematically investigated to optimize the reaction and provide insight into its mechanism. The reaction is believed to follow a different pathway than that of traditional heterogeneous catalysts, which likely is responsible for the excellent yield and selectivity obtained with the Pd nanocatalysts. The relationship between the nanoparticles' structure and their activity and stability also was explored; in general, the smaller and more uniform the nanoparticles size, the higher the activity and stability obtained.

#### Acknowledgments

This work was supported by the National Science Foundation of China (projects 20533010, 20773005, J0630421). The

authors thank Nanjing Huagong Co. Ltd. for the generous gift of the limonene used in this study.

#### Supplementary material

The online version of this article contains additional supplementary material.

Please visit DOI: [10.1016/j.jcat.2008.01.003](https://doi.org/10.1016/j.jcat.2008.01.003).

#### References

- [1] A. Corma, S. Iborra, A. Velty, *Chem. Rev.* 107 (2007) 2411.
- [2] K.A.D. Swift, *Top. Catal.* 27 (2004) 143.
- [3] J.M. Derfer, M.M. Derfer, in: *Kirk-Othmer Encyclopedia Chem. Technol.*, vol. 22, John Wiley & Sons, Inc., New York, 1978, p. 709.
- [4] P. Lesage, J.P. Candy, C. Hirigoyen, F. Humblot, J.M. Basset, *J. Mol. Catal. A Chem.* 112 (1996) 431.
- [5] D. Buhl, D.M. Roberge, W.F. Hölderich, *Appl. Catal. A Gen.* 188 (1999) 287.
- [6] P.A. Weyrich, W.F. Hölderich, M.A. Daelen, A.M. Gorman, *Catal. Lett.* 52 (1998) 7.
- [7] P.A. Weyrich, W.F. Hölderich, *Appl. Catal. A Gen.* 158 (1997) 145.
- [8] R.J. Grau, P.D. Zgolicz, C. Gutierrez, H.A. Taher, *J. Mol. Catal. A Chem.* 148 (1999) 203.
- [9] H. Pines, R.C. Olberg, V.N. Ipatieff, *J. Am. Chem. Soc.* 74 (1952) 4872.
- [10] R.P. Linstead, K.O.A. Michaelis, S.L.S. Thomas, *J. Chem. Soc.* (1940) 1139.
- [11] R.C. Palmer, *Ind. Eng. Chem.* 34 (1942) 1028.
- [12] R. Neumann, M. Lissel, *J. Org. Chem.* 54 (1989) 4607.
- [13] D.J. Cole-Hamilton, *Science* 299 (2003) 1702.
- [14] R.T. Baker, W. Tumas, *Science* 284 (1999) 1477.
- [15] D.B. Zhao, M. Wu, Y. Kou, E.Z. Min, *Catal. Today* 74 (2002) 157.
- [16] N. Yan, C. Zhao, C. Luo, P.J. Dyson, H. Liu, Y. Kou, *J. Am. Chem. Soc.* 128 (2006) 8714.
- [17] X.D. Mu, J.Q. Meng, Z.C. Li, Y. Kou, *J. Am. Chem. Soc.* 127 (2005) 9694.
- [18] C. Zhao, H.Z. Wang, N. Yan, C.X. Xiao, X.D. Mu, P.J. Dyson, Y. Kou, *J. Catal.* 250 (2007) 33.
- [19] C.X. Xiao, H.Z. Wang, X.D. Mu, Y. Kou, *J. Catal.* 250 (2007) 25.
- [20] M. Zou, X.D. Mu, N. Yan, Y. Kou, *Chin. J. Catal.* 28 (2007) 389.
- [21] T. Wang, C.X. Xiao, L. Yan, L. Xu, J. Luo, H. Shou, Y. Kou, H. Liu, *Chem. Commun.* (2007) 4375.
- [22] J.A. Widegren, R.G. Finke, *J. Mol. Catal. A Chem.* 191 (2003) 187.
- [23] M.T. Reetz, G. Lohmer, *Chem. Commun.* (1996) 1921.
- [24] A. Roucoux, J. Schulz, H. Patin, *Adv. Synth. Catal.* 345 (2003) 222.
- [25] T. Teranishi, M. Miyake, *Chem. Mater.* 10 (1998) 594.
- [26] J.L. Pellegatta, C. Blandy, R. Choukroun, C. Lorber, B. Chaudret, P. Lecante, E. Snoeck, *New J. Chem.* 27 (2003) 1528.
- [27] V. Kogan, Z. Aizenshtat, R. Neumann, *New J. Chem.* 26 (2002) 272.
- [28] A.P. Umpierre, G. Machado, G.H. Fecher, J. Morais, J. Dupont, *Adv. Synth. Catal.* 347 (2005) 1407.
- [29] W.T. Reichle, *J. Catal.* 94 (1985) 547.
- [30] F. Lu, J. Liu, J. Xu, *Adv. Synth. Catal.* 348 (2006) 857.
- [31] F. Lu, J. Liu, J. Xu, *J. Mol. Catal. A Chem.* 271 (2007) 6.